POLITECNICO DI TORINO
Repository ISTITUZIONALE

ON THE USE OF STOCHASTIC RESONANCE FOR FAULT DETECTION IN SPUR GEARBOXES

(Article begins on next page)

19 April 2024

ON THE USE OF STOCHASTIC RESONANCE FOR FAULT DETECTION IN SPUR GEARBOXES

Clement U MBA, Stefano MARCHESIELLO, Alessandro FASANA, Luigi GARIBALDI

DIRG – Politecnico di Torino, Corso Duca degli Abruzzi, 24, 10129 Torino, Italy.

clement.mba@polito.it, stefano.marchesiello@polito.it, alessandro.fasana@polito.it, luigi.garibaldi@polito.it

Abstract

This study demonstrates how a time domain data based non-linear approach known as Stochastic Resonance (SR) can be effectively used for fault detection in spur gearboxes. SR has just been used recently for fault diagnosis in mechanical systems with a focus on faulty systems. This paper examines the behaviour of SR when it is applied to healthy systems, in particular a healthy gearbox and explores approaches like residual signal and filtered signal computations to aid in the containment of false alarms while improving overall results. Although SR is a time domain procedure, its results also extend to the frequency domain.

Keywords: Stochastic Resonance, false alarms, residual signals, filtered signals

1. INTRODUCTION

Maintenance activities are periodically performed on machineries as part of cost saving and safety measures. There is no doubt that vibration based condition monitoring plays a key part in maintenance which is why numerous techniques for performing vibration based condition monitoring exist, some of which are quite new.

Stochastic Resonance (SR) has only been used recently for fault detection in mechanical systems. SR is a phenomenon that occurs in non-linear systems whereby hidden information such as a weak signal is amplified and made more obvious using noise. Generally, a periodic input, inherent noise and system threshold are required for SR to occur. These features cause a resonance like behaviour response of the non-linear system as a function of the noise, thus the name Stochastic Resonance [4]. The uniqueness of SR lies in its ability to capitalize on the noise that is inherent in a system [17]. Moreover it has a simple equation that is quite easy to apply. However, the downside to using SR is that there is no clear theory for the selection of SR parameters although there are different methods currently in use. Additionally, SR computing time takes a while especially for large samples of vibration signal. Nevertheless, researches that have been conducted so far on the application of SR to mechanical systems have shown promising results [8, 10-12] and thus, the application of SR remains an area of significant interest. Marchesiello et al. [11] used SR to enhance fault detection in bearings and also presented a method for the selection of SR parameters. By using numerical simulations, Mba et al. [12] showed that SR can be used for fault detection in spur gears. Leng et al. [10] used SR for the

diagnosis of electromotor faults and metal cutting process. Lei et al. [8] applied SR to fault identification in a planetary gearbox by using an ant colony algorithm to optimize the parameters of SR. Li et al. [9] combined SR with sliding windows for identifying impulse signals of a gearbox. While all the researches mentioned present interesting results, there is still limited research on how well SR works when applied to healthy mechanical systems. Majority of available studies only focus on faulty systems.

This paper addresses the issues of SR behaviour when it is applied to vibration signals from a healthy gearbox. In addition, it validates the numerical simulation results in [12] and also attempts to establish the suitability of SR as a diagnostic tool. Also, a short assessment of the most common diagnostic tools for gearbox condition monitoring is done with their results compared. The idea is to show that SR has the potential to act as an amplifier not only for kurtosis, but also for some of the other gearbox diagnostic tools. Furthermore, the effect of SR is shown in both time and frequency domain for numerical simulations and experimental data.

2. STOCHASTIC RESONANCE

SR is a non-linear time domain approach that was first used within the framework of the earth's climate [1]; however its application has been extended to other fields such as physics, chemistry, finance, biology and engineering [13]. Going by its broad definition, SR describes a situation where the existence of noise in a non-linear system is used to strengthen the system's output in terms of its Signal to Noise Ratio (SNR). In other words, rather than degradation in system performance because of

noise, SR works with noise and uses noise to its advantage. It is governed by the non-linear dynamic equation:

$$\frac{dx}{dt} = -\frac{dU(x)}{dx} + s(t) + n(t) \qquad (1)$$

where $U(x)$ is the potential function, $s(t)$ is the input signal and $n(t) = \sqrt{2D}\varepsilon$ is the input noise with D being the noise intensity and ε the Gaussian noise. $U(x)$ which is a reflection-symmetric quartic potential [4] is given as

$$U(x) = -\frac{1}{2}ax^2 + \frac{1}{4}bx^4 \qquad (2)$$

Where a and b are the non-linear system parameters. Accordingly, Eq. (1) can be rewritten as

$$\frac{dx}{dt} = ax - bx^3 + s(t) + n(t) \qquad (3)$$

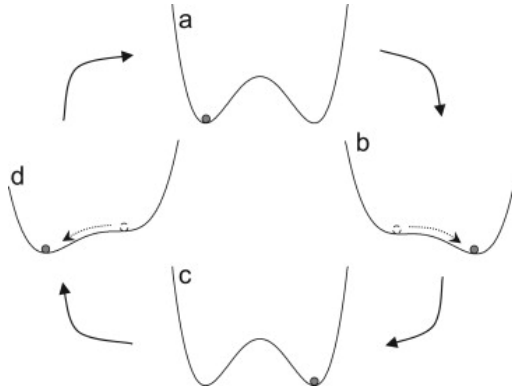In order to illustrate how this phenomenon works, let's consider figure 1.

Fig. 1. Bistable system showing Brownian particle motion in the presence of a periodic input signal and noise [11]

The figure shows a double well symmetric potential with four different states a, b, c and d. Let's consider a ball in one of the wells of each potential. When a periodic input signal is applied to the potential in a, both the left side and the right side wells modulate but this modulation does not cause the ball to move to the next well. When a certain amount of noise is properly combined with the periodic input signal and applied to the potential, the addition of noise gives the particle enough energy to move between wells. This is what happens in b, c and d. In the absence of both the periodic input signal and noise, the behaviour of the particle depends on initial conditions [4]. Assuming

that "a" in figure 1 is the original state of a non-linear system, the parameters a and b in equation 3 can be tuned in such a way that the particle jumps to the height of the barrier between the wells without getting into the right side well but rather returns to left side well. This event produces a spike that can be quantified by a performance indicator such as kurtosis and can be used to detect tiny or hidden impulses in a noisy signal. Figure 2 demonstrates such a scenario.
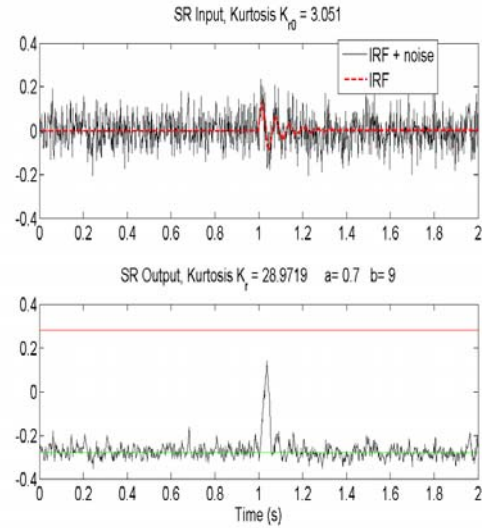

Fig. 2. Example showing results that can be obtained when a and b are well-tuned [11]. Note that in the bottom figure, the green horizontal line represents the left side of the well in figure 1 and the red horizontal line represents the right side of the well in the same figure.

The top of figure 2 shows an Impulse Response Function (IRF) submerged in noise which represents $s(t) + n(t)$ in equation 3. The SR output which is given by x in equation 3 and shown at the bottom of figure 2 is obtained when equation 3 is solved numerically with parameters a and b well-tuned. The green horizontal line represents the left side of the well in figure 1 which is defined as $-\sqrt{\frac{a}{b}}$ while the red horizontal line represents the right side of the well in the same figure and it is defined as $\sqrt{\frac{a}{b}}$. The vertical distance from either the green line or the red line to zero at the bottom of figure 2 represents the height of the barrier or threshold. In this particular scenario, the parameters a and b are tuned in such a way that the SR output gets to the edge of getting into the right side well (horizontal red line) after crossing the threshold but does not, instead it returns to the left side well (horizontal green line). This results in a

clear amplification of the impulse as can be seen at the bottom of figure 2.

Eq. 3 is quite suitable for small parameter systems, i.e. amplitude and frequency of the input signal <<1 and noise intensity D<<1. But realistic systems are usually large parameter systems, i.e amplitude and frequency of the input signal >>1 and noise intensity D>>1. Because of this, large parameter systems are subjected to pre-processing techniques like scale normalization, modulation, re-scaling frequency, etc. [8] in order to make them meet the requirements of small parameter systems. Like the previous work in [12], re-scaling frequency is used in this paper to ensure that the gearbox system meets the requirements needed for the functionality of SR. Furthermore, queries come up when it comes to the issue of how best to tune the parameters a and b. Although there are researches both present and ongoing that show how best to go about this matter [2, 8, 11, 16], what has been shown to be quite effective and simple to apply is normalizing the input signal with a standard deviation of 0.07 before defining a fixed range for $a \in [0.1,1]$ with an interval of 0.1 and $b \in [1,11]$ with an interval of 1. Then a search is performed within the defined ranges to find the maximum kurtosis. Finally, the combination of a and b that gives the maximum kurtosis within the defined range is selected and used to find the corresponding SR output.

2.1. Numerical Simulations and Analyses

The dynamic response of a single stage reduction spur gearbox is simulated by using the equations of motion described in [5]. In [5], it is shown that friction has negligible influence on the simulated dynamic response so it is ignored here just like in the previous work in [12]. The simulation takes varying meshing stiffness into account which changes in value as the load bearing capacity of the meshing gears changes during rotation. The load bearing capacity reduces in the presence of a fault and the amount by which it is reduced depends on the severity of the fault. Different severities of fault are included in the simulation by using different time histories of the varying meshing stiffness. A simple transmission part between the source of vibration and the transducer is also taken into account with its natural frequency selected as 176 Hz based on its method of support [3] and a damping ratio of 0.05.

The top of figure 3a shows a generated acceleration data submerged in Gaussian noise with a certain amount of fault. The data is for the steady part of the generated acceleration signal and is obtained for 5 revolutions of both the pinion and gear. Again in the bottom of figure 3, the green line in the SR output plot represents the negative side of the potential shown in figure 1 while the red line

represents the right side of the potential. The purple line, which shows where the fault is supposed to appear, is generated from the varying meshing stiffness time histories.
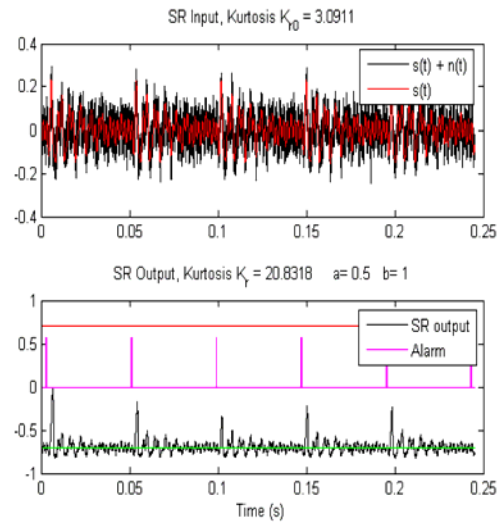

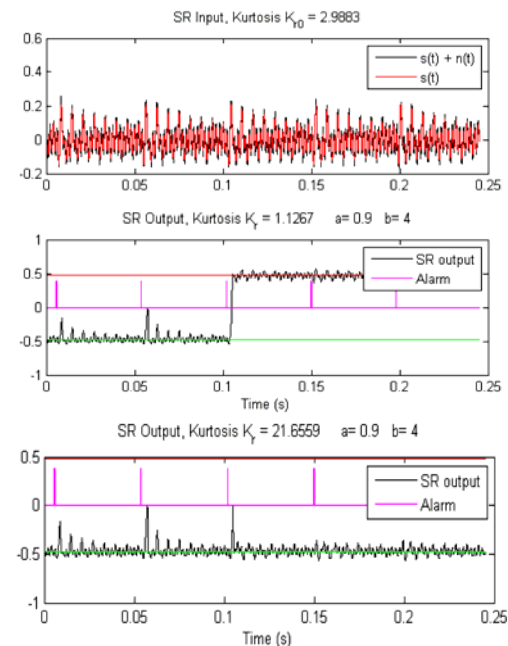Fig. 3a. Comparison of SR input and SR output with reference fault.

Fig. 3b. Comparison of SR input and SR output with fault severity reduced by 50%. The bottom plot is obtained after "rectification" of the middle plot
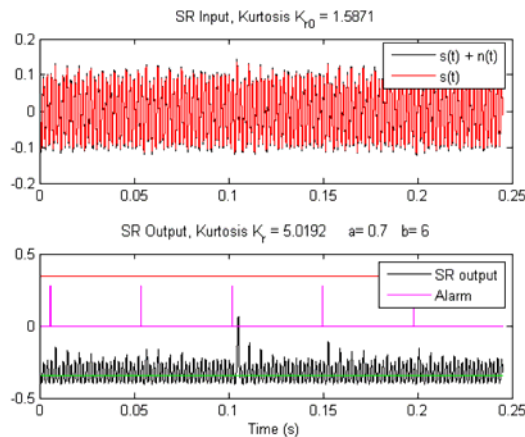
Fig. 3c. Comparison of SR input and SR output
with fault severity reduced by 90%.

As can be seen from figure 3a, SR raises the impulses present in the SR input as quantified by the kurtosis. This goes on even as fault severity is reduced in figure 3b. In this figure, "rectification" is applied to the first SR output plot to obtain the second SR output plot. "Rectification" was recently investigated by the authors [11, 12] and basically, it helps to keep the SR output bounded between the negative well of the potential and zero. This helps to prevent biased results like the one in the first SR output plot of figure 3b, and in majority of cases, it enhances SR output. When the fault severity is greatly reduced as shown in the SR input plot of figure 3c, SR still remains effective as can be seen in the SR output plot of the same figure. In all these cases, kurtosis has been used as a performance indicator.

With a view to showing the effect of SR as a possible amplifier for other performance indicators, figure 4 shows the changes that statistical features for gearbox condition undergo for both SR and non-SR signals as the fault severity progresses from 1 – 4 on the x axis with 1 being the healthy case, 2 being a small fault case, 3 being a medium fault case and 4 being a large fault case. Figure 4a shows the changes that occur when the statistical indicators are applied directly to either the raw signal, its Time Synchronous Average (TSA), residual or difference signal and figure 4b shows the changes that occur when the statistical indicators are applied to the output of the SR system after the raw signal is passed through the SR system. As can be seen with some of the indicators, SR tends to amplify the absolute changes that occur in all or some stages of fault growth. This is particularly true for the kurtosis, crest factor, FM0, FM4, M6A, NB4, M8A, ENA4 and energy operator [7,14,15]. In general, the kurtosis and FM0 provide the clearest indication of these changes; however, the overall amplification is greater in the kurtosis than in any of the other indicators. This either shows that kurtosis might be the most fitting indicator for SR in the time domain, or could be as a result of basing the selection of the parameters a

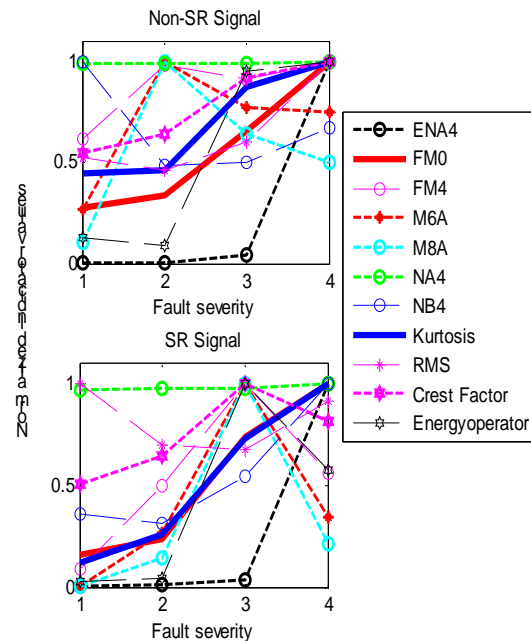and b on kurtosis maximization. Further research will need to be done to verify this.

Fig. 4 Comparison of the changes in the most common gearbox fault diagnosis statistical features. On the x axis, 1 = healthy case, 2 = small fault case, 3= medium fault case and 4 = large fault case (a) non-SR Signal (b) SR Signal

The numerical simulation is extended with the addition of a pulse generator. The reason for this is to be able to generate a signal that is equivalent to the tachometer signal generated in real life scenarios which is very useful for computation of the TSA signal. Other factors like the transmission part and Gaussian noise are still taken into account. We note here that the addition of Gaussian noise to the acceleration signal leads to different realizations of a "modified acceleration signal." From here onward in this paper, the same realization of modified acceleration signal is used for all analyses conducted. Moreover, more focus is on the frequency domain results which reveal more information than the time domain results.

Figure 5 shows the obtained results when the frequency spectra is computed for the time domain results with and without SR with a driving shaft speed of 1248 revolutions per minute (rpm), and tooth meshing frequency of 478 Hz. The magenta lines in the figures show where the sidebands are supposed to be theoretically. As expected, the sideband amplitudes of the non-SR signal reduce as the fault severity reduces.

In the healthy case of figure 5 (a), there is no amplification of sidebands in the SR signal. However, a few more spikes can be seen in the SR signal when compared to the non-SR signal. In figures 5 (b) & (c), the effect of SR on the modified acceleration signal is not very obvious in the

(a)

PSD of SR Signal

PSD of non-SR Signal

(b)

PSD of SR Signal

PSD of non-SR Signal

(c)

PSD of SR Signal

PSD of non-SR Signal

(d)

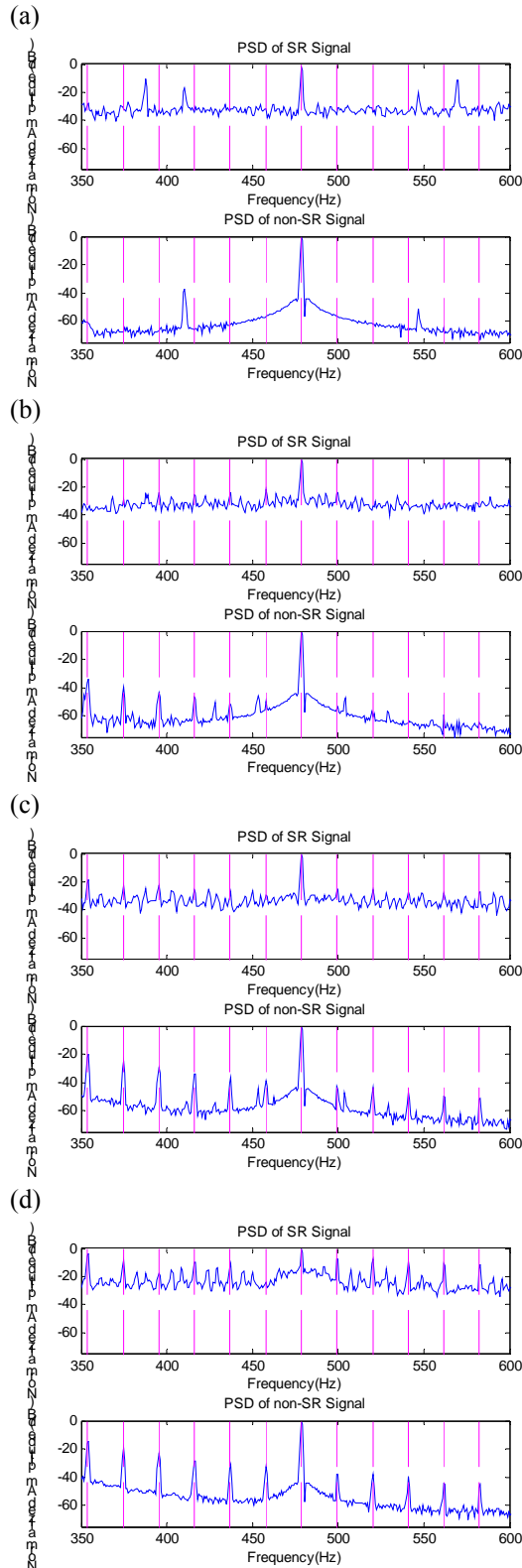PSD of SR Signal

PSD of non-SR Signal

Fig. 5. Vibration spectrum of a single stage reduction 1248-rpm gearbox (a) healthy case (b) fault reduced by 90% (c) fault reduced by 50% (d) reference fault

frequency domain unlike the time domain results in [12]. The effect of SR is quite evident in figure 5 (d) as there are clear indications of amplification of the sidebands in the SR signal especially after the

meshing frequency. The sideband amplitudes are more distinct in the non-SR signals than the SR signals, which appear noisy at best. In the figures, it seems easier to differentiate the healthy gear from the faulty gear by looking at the non-SR signal which could bring one to the conclusion that the effect of SR on gear data is not very pronounced in the frequency domain.
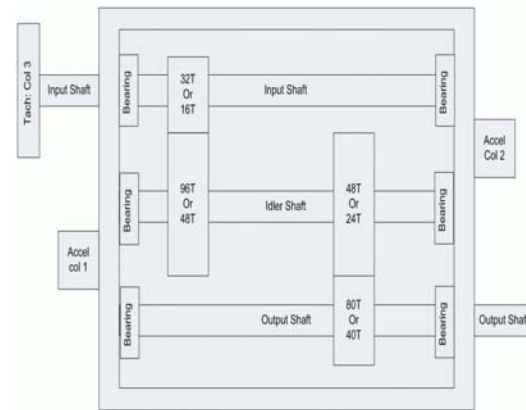
2.2. Experimental Results and Analyses

Fig. 6 Schematic diagram of a double stage reduction gearbox [6]

The experimental data used for validating the numerical results is obtained from PHM dataset 2009 [6] where a double stage reduction gearbox with different fault severities is run at different speeds with both high and low loads. The schematic of the gearbox is shown in figure 6. There is a completely healthy case, another case where there is a chipped gear tooth and another case where there is a broken gear tooth. In addition, the runs are repeated twice for each load and speed. Here, our analysis focuses on the first-run data with an input shaft speed of 30 Hz and high load as well as data from channel 2 and the spur gear setup. Furthermore, SR is applied to the healthy case, chipped tooth case and the broken tooth case with the results given below.

Figures 7 – 9 show the vibration spectra obtained for the spur gearbox with the corresponding SR signals on the bottom side (i.e. third and fourth rows) of each figure and non-SR signals on the top (i.e. first and second rows) of each plot. Each plot in the figures has an upper section corresponding to the spectrum for the lower meshing frequency range and a lower section corresponding to the spectrum for the upper meshing frequency range. The red and magenta lines represent the theoretical position of the sidebands around their corresponding fundamental frequencies.

8

DIAGNOSTYKA, Vol. 18, No. 3 (2017)
MBA CU, MARCHESIELLO S, FASANA A, GARIBALDI L.: On the use of stochastic resonance for ...
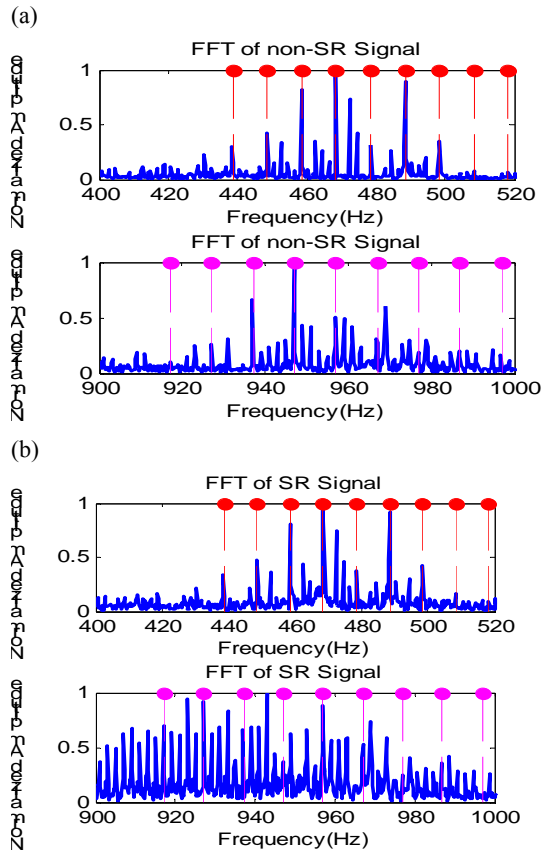
(a)

(b)

Fig. 7 Non-SR and SR vibration spectrum of a 1800 rpm double stage reduction spur gearbox – healthy tooth case (a) lower meshing frequency range (b) upper meshing frequency range
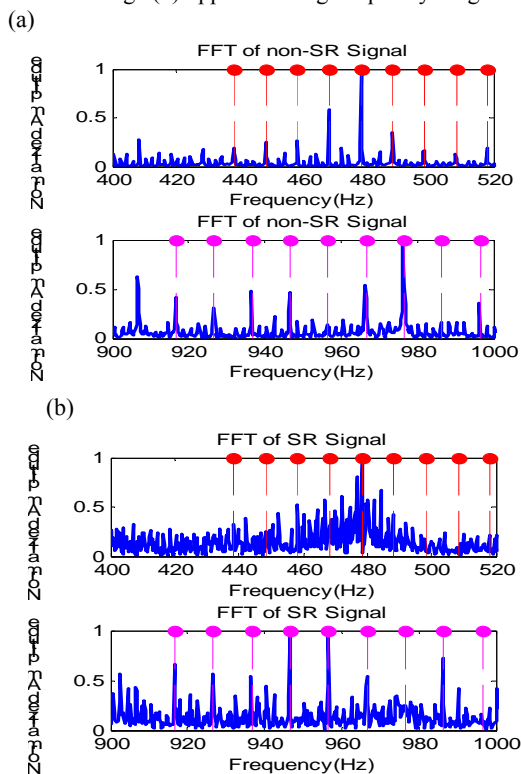
(a)

(b)

Fig. 8 Non-SR and SR vibration spectrum of a 1800 rpm double stage reduction spur gearbox – chipped tooth case (a) lower meshing frequency range (b) upper meshing frequency range
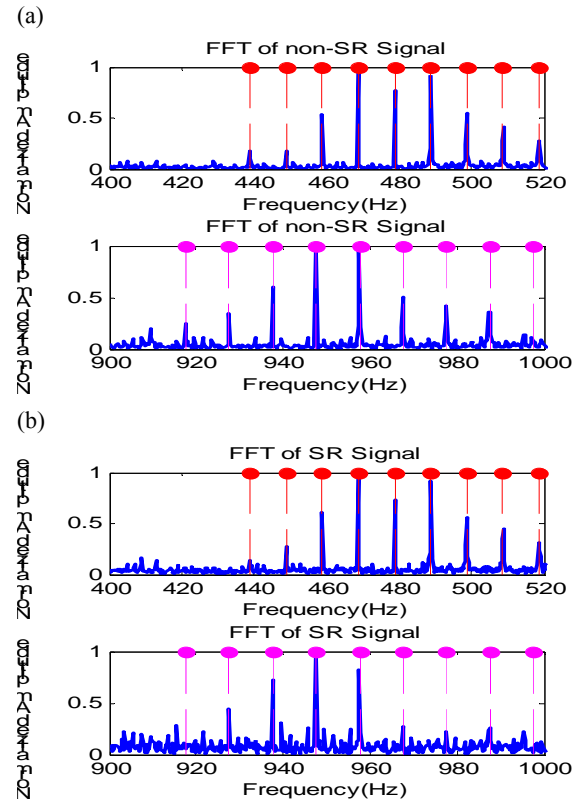
(a)

(b)

Fig. 9 Non-SR and SR vibration spectrum of a 1800 rpm double stage reduction spur gearbox – broken tooth case (a) lower meshing frequency range (b) upper meshing frequency range

In the healthy case of figure 7, there is not a lot of difference between the non-SR and SR signal in the lower meshing frequency range, nevertheless, there is a huge amplification of sidebands in the higher meshing frequency range. In figure 8, the SR signal appears noisy in the lower meshing frequency range while there is an amplification of eccentric gear sidebands in the higher meshing frequency range. Comparing the non-SR signal and SR signal of figure 9, there is no obvious difference between them, both in the lower and higher meshing frequency range.

In an overall sense, there almost always seems to be amplification in the SR signals with the amplifications in the higher meshing frequency range looking more noticeable and noisy. This also applies to the healthy signals, which could be because of all the frequencies contained in the raw signal. The amplification of sidebands in the healthy signals appears to be more apparent in the experimental case than the numerical case. It is a well-known fact that experimental data have more noise, vibration and complexity and as a result, they could be more difficult to analyse properly. This implies that it might be imperative to pre-process or "simplify" experimental data signals before applying SR in order to obtain the best results. Pre-processing could involve residual signal or high-pass filtered signal computation as illustrated in the following sections, or any other technique deemed suitable.

3. APPLYING STOCHASTIC RESONANCE TO RESIDUAL SIGNALS

The residual signal is obtained by removing the meshing frequencies and the shaft frequencies along with their harmonics from the original Time Synchronous Averaged (TSA) signal [7, 14, 15].

$$r = x(t) - x_r(t) \qquad (5)$$

where r is the residual signal, $x(t)$ is the original TSA and $x_r(t)$ is the signal containing the meshing frequencies, shaft frequencies and their harmonics. When the first order sidebands are removed from the residual signal, a difference signal is formed.

$$d = r - (f_m \pm \omega) \qquad (6)$$

where d is the difference signal, f_m is the signal meshing frequency and ω is the shaft frequency. Both the residual and difference signal were proposed in order to better observe the changes that occur in a vibration signal [14].

In our computation, the frequencies mentioned are removed from the TSA of the exact realization of non-SR modified acceleration signals that are shown in figure 5 to obtain the non-SR signals shown in figures 10. Clearly, the sidebands are more evident in the signals and it is easier to understand them.

All the amplitudes in figure 10 are displayed in dB scale for more clarity. The SR and non-SR signals of figure 10 (a) are almost the same, which means that false alarms are almost non-existent in this scenario. In figure 10 (b), the sidebands in the SR signal are amplified randomly while in figure 10 (c), the amplification is done after 400 Hz. In figure 10 (d), the amplitude of the sidebands relative to that of the fundamental frequency is higher in the SR signal than in the non-SR signal.

When the same procedure is applied to the experimental data of the spur gear setup, the results obtained agree well with the numerical results as seen in figures 11 – 13. In the healthy case, both the SR and non-SR signals are similar just like the numerical simulation result. The frequency spikes are evident in the SR signal of figure 12 especially in the higher meshing frequency range. The spikes that are present in the lower meshing frequency range are most likely due to the eccentric gear which are not as conspicuous as the spikes in the higher meshing frequency range which are most likely due to the chipped gear. In figure 13 where there is an eccentric gear and a gear with broken tooth, the frequency spikes are very evident in both
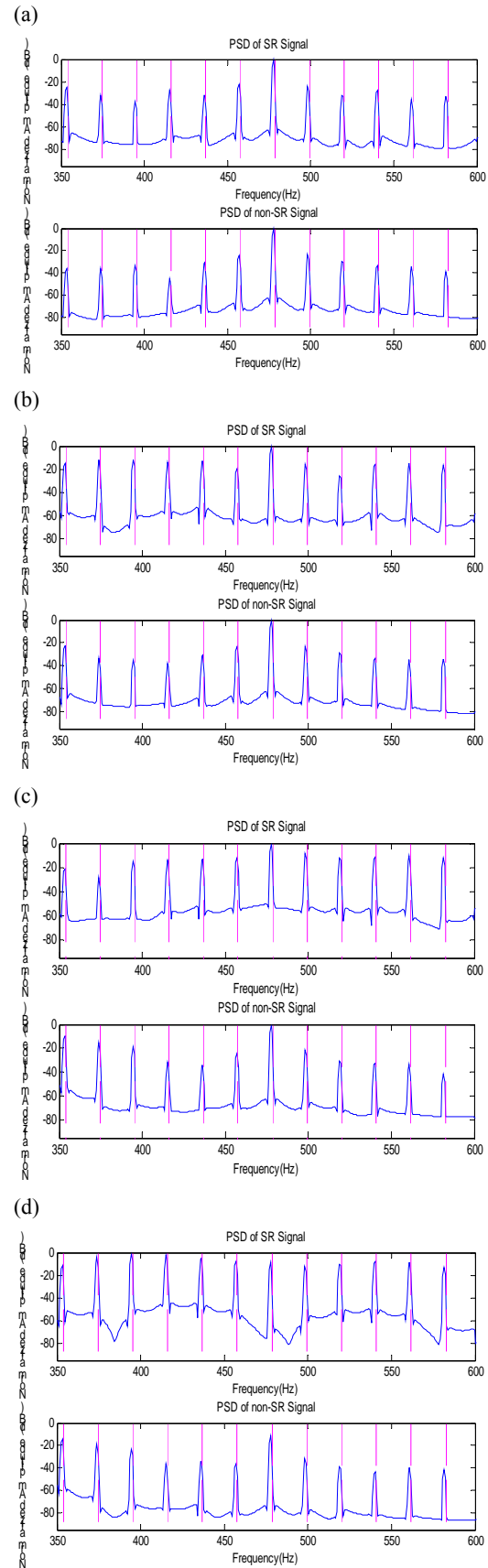

Fig. 10 Residual signal vibration spectrum of a single stage reduction 1248-rpm gearbox (a) healthy case (b) fault reduced by 90% (c) fault reduced by 50% (d) reference fault
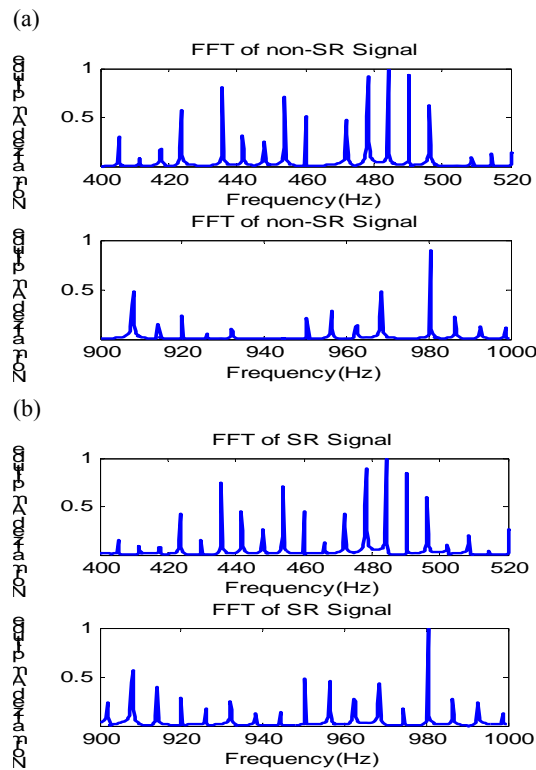
(a)

(b)

Fig. 11 Non-SR and SR residual signal vibration spectrum of a 1800 rpm double stage reduction spur gearbox – healthy tooth case (a) lower meshing frequency range (b) upper meshing frequency range
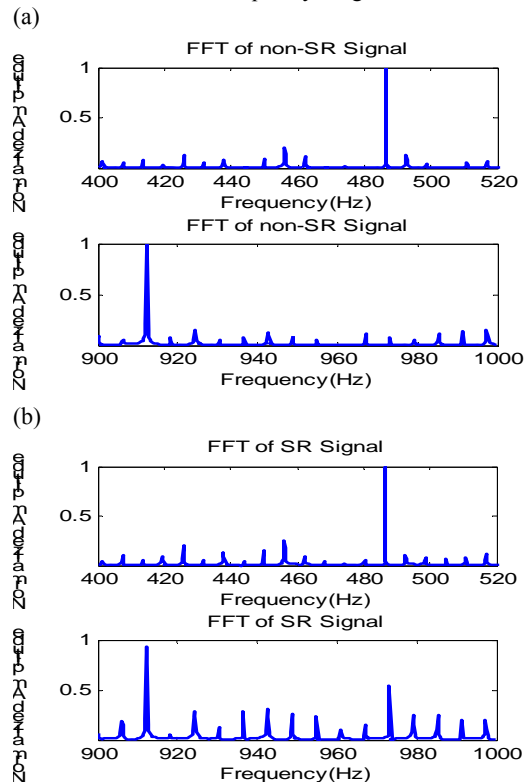
(a)

(b)

Fig. 12. Non-SR and SR residual signal vibration spectrum of a 1800 rpm double stage reduction spur gearbox – chipped tooth case (a) lower meshing frequency range (b) upper meshing frequency range
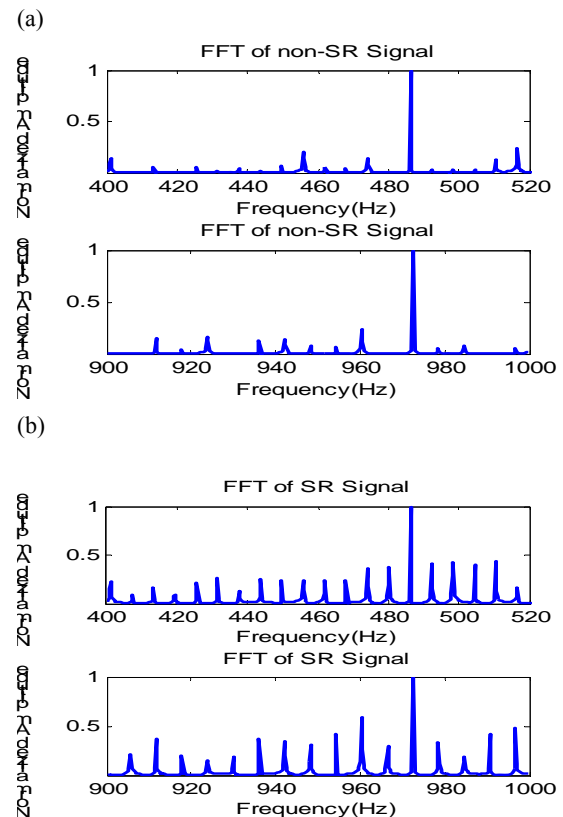
(a)

(b)

Fig. 13 Non-SR and SR residual signal vibration spectrum of a 1800 rpm double stage reduction spur gearbox – broken tooth case (a) lower meshing frequency range (b) upper meshing frequency range

the lower and upper meshing frequency range. The frequency spikes in the lower meshing frequency range are due to the eccentric and broken tooth gears while the spikes in the upper meshing frequency range are most likely as a result of the harmonics of the spikes in the lower meshing frequency range. It should be noted that the frequency spacing of the non-SR signal is not regular while that of the SR signals is regular and spaced at 6 Hz corresponding to the speed of the output shaft. This is because the TSA was computed only for the output shaft before computing the residual signal.

4. APPLYING STOCHASTIC RESONANCE TO HIGH-PASS FILTERED SIGNALS

In the time domain, the SR output of the experimental data of the healthy gears gives a high kurtosis. This is not the case for the numerical simulations, which gives a low kurtosis when SR is applied to the healthy gear signal. As indicated earlier, the most reasonable explanation for this phenomenon is that experimental data has more vibration, noise and complexity that make it difficult to properly examine it. In this section, a high-pass Butterworth filter with a proper cut-off

frequency is used to make the data to be analysed "less complex." The cut-off frequency of the filter is selected in such a way that the kurtosis of the filtered signal is slightly less than the kurtosis of the original signal using the healthy case as reference. This is depicted schematically in figure 14.
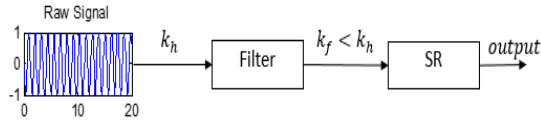

Fig. 14 Schematic diagram showing a possible way of choosing the high-pass filter cut-off frequency

The raw signal in figure 14 is a healthy signal, which was used as a reference because SR tends to always amplify the numerical value of the kurtosis and we are trying to keep the initial kurtosis as low as possible. k_h is the kurtosis of the healthy signal and k_f is the kurtosis of the filtered signal. The value of the cut-off frequency of the filter that coincides with k_f about 90% of k_h is selected in this case. It should be noted that the primary goal here is to contain false alarms in the time domain.

Using this procedure, 0.216 is selected as the normalized cut-off frequency of the high-pass Butterworth filter. The top plot of figures 15 – 17 displays the raw signals, the middle plot displays the SR output without filtering and the bottom plot displays the SR output after filtering. As always, the green line in the second and third plots of each figure corresponds to the negative well of the symmetric double well potential of the SR dynamic system while the red line in the plots corresponds to the positive well of the symmetric double well potential of the SR dynamic system. In figure 15, the kurtosis of the SR output in the bottom plot (c) is much lower than the kurtosis of the SR output in the middle plot (b). In the bottom plot (c) of figures 16 and 17, the kurtosis of the SR output is more amplified when compared with the middle plot (b) of the same figures. These results not only demonstrate that false alarms in the time domain can be contained in SR output when the raw signal is filtered before passing it through the SR dynamic system, but also that SR output can be enhanced as seen in figures 16(c) and 17(c).
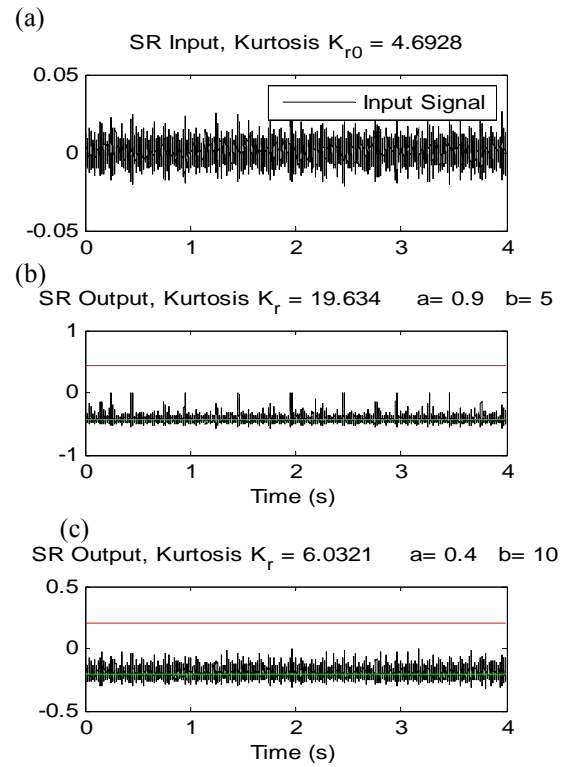

Fig 15. Experimental results for the spur gear setup – healthy case (a) raw signal (b) SR signal (c) filtered SR signal.
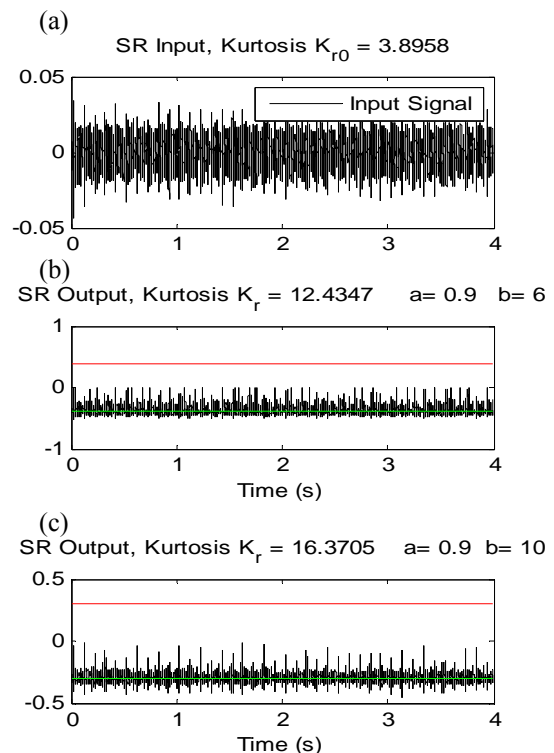

Fig. 16. Experimental results for the spur gear setup – chipped tooth case(a) raw signal (b) SR signal (c) filtered SR signal.
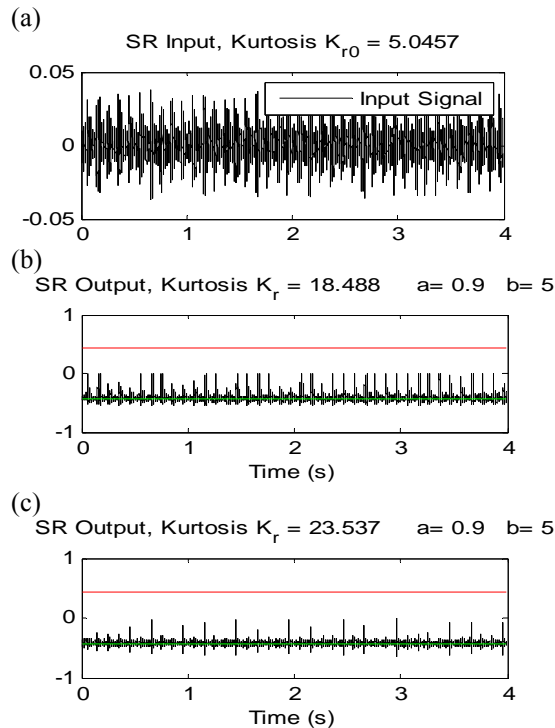
(a)

(b)

(c)

Fig. 17. Experimental results for the spur gear setup – broken tooth case(a) raw signal (b) SR signal (c) filtered SR signal.

4. CONCLUSIONS

There are many vibration-based condition-monitoring techniques amongst which, SR stands out in the sense that it can exploit system noise positively. In addition to amplifying the kurtosis for faulty gears in the time domain, it also acts as an amplifier for other fault detecting statistical features. Although few researches have been done on applying SR to mechanical problems, much of the already done research focuses on faulty cases. In this paper, more attention is given to the effect of SR on data from healthy gearboxes. Analyses conducted in the frequency domain tend to imply that the effect of SR on gearbox acceleration signals is neither clear nor well pronounced. In the time domain on the other hand, while there are no problems when SR is applied directly to data from numerical simulations, misleading results can be obtained when SR is applied directly to experimental data. Based on the complexity of realistic data, which seems to affect SR results, a plausible solution would be to pre-treat data in order to reduce its complexity before applying SR. Two strategies are taken to solve this problem in this work. The first tactic involves computation of the residual signal by removing some defined frequencies from the TSA of the original signal. The second approach involves applying a high-pass filter with a proper cut-off frequency to the original signal. The results obtained when SR is applied to the residual signal and filtered signal, rather than the raw signal look promising as can be seen in the latter part of this paper. A suitable area of future research will be to apply the strategies developed here to other real life datasets.

REFERENCES

1. Benzi R, Sutera A, Vulpiani A. The mechanism of stochastic resonance. Journal of Physics A: mathematical and general. 1981;14(11):L453.
2. Chen XH, Cheng G, Shan XL, Hu X, Guo Q, Liu HG. Research of weak fault feature information extraction of planetary gear based on ensemble empirical mode decomposition and adaptive stochastic resonance. Measurement. 2015;73:55-67.
3. Dickinson S, Warburton G. Vibration of box-type structures. Journal of Mechanical Engineering Science. 1967;9(4):325-38.
4. Gammaitoni L, Hänggi P, Jung P, Marchesoni F. Stochastic resonance. Reviews of modern physics. 1998;70(1):223.
5. Howard I, Jia S, Wang J. The dynamic modelling of a spur gear in mesh including friction and a crack. Mechanical systems and signal processing. 2001;15(5):831-53.
6. http://www.phmsociety.org/references/datasets. 2009 PHM Challenge Competition Data Set. 2009.
7. Lebold M, McClintic K, Campbell R, Byington C, Maynard K. Review of vibration analysis methods for gearbox diagnostics and prognostics. Proceedings of the 54th Meeting of the Society for Machinery Failure Prevention Technology; 2000.
8. Lei Y, Han D, Lin J, He Z. Planetary gearbox fault diagnosis using an adaptive stochastic resonance method. Mechanical Systems and Signal Processing. 2013;38(1):113-24.
9. Li J, Chen X, He Z. Adaptive stochastic resonance method for impact signal detection based on sliding window. Mechanical Systems and Signal Processing. 2013;36(2):240-55.
10. Leng YG, Leng YS, Wang TY, Guo Y. Numerical analysis and engineering application of large parameter stochastic resonance. Journal of Sound and Vibration. 2006;292(3):788-801.
11. Marchesiello S, Fasana A, Garibaldi L. Best parameter choice of Stochastic Resonance to enhance fault signature in bearings. International Conference on Structural Engineering Dynamics; Lagos, Portugal 2015. p. 1-7.
12. Mba CU, Marchesiello S, Fasana A, Garibaldi L. Vibration Based Condition Monitoring of Spur Gears in Mesh using Stochastic Resonance. Surveillance 8 International Conference; Roanne, France 2015. p. 1-15.
13. McDonnell MD, Abbott D. What is stochastic resonance? Definitions, misconceptions, debates, and its relevance to biology. PLoS Comput Biol. 2009;5(5):e1000348.
14. Samuel PD, Pines DJ. A review of vibration-based techniques for helicopter transmission diagnostics. Journal of sound and vibration. 2005;282(1):475-508.
15. Večeř P, Kreidl M, Šmíd R. Condition indicators for gearbox condition monitoring systems. Acta Polytechnica. 2005;45(6).
16. Worden K, Antoniadou I, Marchesiello S, Mba C, Garibaldi L. An illustration of new methods in machine condition monitoring, part 1: stochastic resonance. Journal of Physics: Conference Series 2017, p. 1-10.

17. Yan R, Zhao R, Gao RX. Noise-assisted data processing in measurement science: Part one part 40 in a series of tutorials on instrumentation and measurement. Instrumentation & Measurement Magazine, IEEE. 2012;15(5):41-4.

Clement Uchechukwu Mba has an MSc in Automotive Engineering and is currently doing his PhD in Mechanical Engineering at Politecnico di Torino under the supervision of Prof. Stefano Marchesiello in the Dynamics and Identification Research Group (DIRG). The main focus of his PhD is on developing and applying new tools for the purpose of vibration based fault diagnosis in rotating machinery. His research interests include Condition Monitoring and Fault Identification, System Dynamics Modelling and Simulation, and Control Theory.

Stefano Marchesiello has MSc degree in Mechanical Engineering and a PhD in Applied Mechanics. He is currently an Associated Professor at the Politecnico di Torino and actively works in the Dynamics and Identification Research Group (DIRG). His research interests include Linear and Nonlinear Identification, Condition Monitoring and Structural Health Monitoring, System Dynamics, Modal Analysis, Moving loads.

Alessandro FASANA has MSc degree in Aeronautical Engineering and a PhD in Applied Mechanics. He is currently an Associated Professor at the Politecnico di Torino and actively works in the Dynamics and Identification Research Group (DIRG). His research interests include Condition Monitoring and Structural Health Monitoring, Linear and Nonlinear Identification, System Dynamics, Modal Analysis, Characterization and Modelling of Viscoelastic Materials.

Luigi Garibaldi is Full Professor of Applied Mechanics and Vibrations at Politecnico di Torino, since 2002, he is leading the Dynamics & Identification Research Group (DIRG), whose remarkable research fields are: mechanical vibrations, system identification and diagnostics.
Since 2015 he has been also charged for the Research Direction and PhD program of the INSA Euro-Mediterranean University of Fez, Morocco, last branch of INSA French University Group.
Since 2011 (up to end 2017) he is the Coordinator of the PhD in Mechanical Engineering at Politecnico di Torino. Invited researcher for a many times at ISMCM (Supmeca - Paris) in 1993, 1994, 1998 and 2015, he has also been invited professor at the Université de Technologie de Compiègne (UTC), in 2003 and 2004, and 6 months at ENPC (Ecole Nationale des Ponts et Chaussées) in 2008. Since 2013 he gives yearly seminars on gearbox diagnostics at INSA Centre Val de Loire (France).
Member of Mechanical Systems and Signal Processing (Elsevier) Editorial Board since 2004, and Mechanics and Industry (IOP) since 2014, he is reviewer for the most relevant Journals on vibrations, identification and monitoring. He has organized a few congresses, such as DAMAS (2007 in Turin, 2009 in Beijing and 2013 in Ireland) as well as Surveillance (2004 in Compiègne and 2017 in Fez, Morocco); he is also board member of scientific congress committees (AVE, CMMNO, ICEDyn, VISHNO, *CMSM,* Surveillance, DAMAS).
He has been external examiner, tutor or jury president /member for more than 25 PhD Thesis and HDR in Italy, France and Belgium, as well as reviewer for National Research Projects of Belgium, Canada, Israel, Quatar, France.
He has published more than 150 papers in International reviews and congresses and has been invited, as keynote speaker, at the conferences CMMNO 2014, AVE 2012, XX SÉMINAIRE FRANCO- POLONAIS EN MÉCANIQUE 2012 (Varsovie, Pologne), DAMAS 2011, Marie Curie SICON Event 2009 (Rome, Italy and Liège, Belgium).